

EUR 3557 e

EUROPEAN ATOMIC ENERGY COMMUNITY — EURATOM

**TEMPERATURE AND THERMAL STRESS
DISTRIBUTION IN SMOOTH AND FINNED CANNINGS
DUE TO AXIAL FLUX VARIATIONS**

by

J. REYNEN

1967



ORGEL Program

**Joint Nuclear Research Center
Ispra Establishment — Italy**

Technology

LEGAL NOTICE

This document was prepared under the sponsorship of the Commission of the European Atomic Energy Community (EURATOM).

Neither the EURATOM Commission, its contractors nor any person acting on their behalf:

Make any warranty or representation, express or implied, with respect to the accuracy, completeness, or usefulness of the information contained in this document, or that the use of any information, apparatus, method, or process disclosed in this document may not infringe privately owned rights; or

Assume any liability with respect to the use of, or for damages resulting from the use of any information, apparatus, method or process disclosed in this document.

This report is on sale at the addresses listed on cover page 4

at the price of FF 6.—	FB 60	DM 4.80	Lit. 750	Fl. 4.30
------------------------	-------	---------	----------	----------

When ordering, please quote the EUR number and the title, which are indicated on the cover of each report.

Printed by Van Muyswinkel
Brussels, September 1967

This document was reproduced on the basis of the best available copy.

EUR 3557 e

TEMPERATURE AND THERMAL STRESS DISTRIBUTION IN SMOOTH AND FINNED CANNINGS DUE TO AXIAL FLUX VARIATIONS by J. REYNEN

European Atomic Energy Community — EURATOM
ORGEL Program
Joint Nuclear Research Center — Ispra Establishment (Italy)
Technology
Brussels, September 1967 - 44 Pages - 14 Figures - FB 60

Temperature and thermal stress distributions due to thermal neutron flux peaking near the end plugs of fuel rods are determined for both smooth and finned cannings.

The theory has been programmed on a digital computer. The code, named ATEAS, handles empirical flux distributions defined at a number of discrete points by assuming a linear flux distribution between adjacent points.

EUR 3557 e

TEMPERATURE AND THERMAL STRESS DISTRIBUTION IN SMOOTH AND FINNED CANNINGS DUE TO AXIAL FLUX VARIATIONS by J. REYNEN

European Atomic Energy Community — EURATOM
ORGEL Program
Joint Nuclear Research Center — Ispra Establishment (Italy)
Technology
Brussels, September 1967 - 44 Pages - 14 Figures - FB 60

Temperature and thermal stress distributions due to thermal neutron flux peaking near the end plugs of fuel rods are determined for both smooth and finned cannings.

The theory has been programmed on a digital computer. The code, named ATEAS, handles empirical flux distributions defined at a number of discrete points by assuming a linear flux distribution between adjacent points.

EUR 3557 e

EUROPEAN ATOMIC ENERGY COMMUNITY — EURATOM

**TEMPERATURE AND THERMAL STRESS
DISTRIBUTION IN SMOOTH AND FINNED CANNINGS
DUE TO AXIAL FLUX VARIATIONS**

by

J. REYNEN

1967



ORGEL Program

Joint Nuclear Research Center
Ispra Establishment — Italy

Technology

Summary

Temperature and thermal stress distributions due to thermal neutron flux peaking near the end plugs of fuel rods are determined for both smooth and finned cannings.

The theory has been programmed on a digital computer. The code, named ATEAS, handles empirical flux distributions defined at a number of discrete points by assuming a linear flux distribution between adjacent points.

KEYWORDS

FUEL CANS
THERMAL STRESSES
THERMAL NEUTRONS
TEMPERATURE

DISTRIBUTION
PROGRAMMING
CONFIGURATION
FINS

CONTENTS

	Page
1. INTRODUCTION	5
2. TEMPERATURE DISTRIBUTION FOR GIVEN FLUX DISTRIBUTION	5
3. THERMAL STRESSES FOR A GIVEN TEMPERATURE DISTRIBUTION	7
4. THERMAL STRESSES FOR GIVEN FLUX DISTRIBUTION	9
5. NUMERICAL METHODS	11
6. NUMERICAL APPLICATION TO A G 19 FINNED CANNING	16
7. CONCLUSION AND FINAL REMARKS	19
REFERENCES	21
NOMENCLATURE	22
APPENDIX 1	23
APPENDIX 2	27
APPENDIX 3	33
FIGURES	37

TEMPERATURE AND THERMAL STRESS DISTRIBUTION IN SMOOTH
AND FINNED CANNINGS DUE TO AXIAL FLUX VARIATIONS (+)

1. INTRODUCTION

Axial flux variations near the end plugs of fuel rods cause rather accentuated temperature variations, resulting in important thermal stresses. This paper deals with the determination of such temperature and thermal stress distributions. Special attention has been paid to numerical methods in order to handle empirical thermal neutron flux distributions. For that purpose the theory has been programmed on a digital computer (ATEAS⁺⁺).

For the determination of the stresses, the classical theory of symmetrically loaded thin cylinders has been employed. In appendix 2 a correction for finned cannings is presented.

In chapter 6, the thermal stress distribution for an ORGEL type of canning (G 19), as calculated by ATEAS, is presented.

2. TEMPERATURE DISTRIBUTION FOR GIVEN FLUX DISTRIBUTION

The differential equation governing the axial heat transport in the canning can be written as (see appendix 1):

$$\frac{d^2T}{dx^2} - m^2T = -\frac{m^2}{h} q \quad (1)$$

The homogeneous solution of (1) is given by:

$$T = A e^{mx} + B e^{-mx} \quad (2)$$

As can be seen from (2), the homogeneous solution only plays a part near boundaries. The perturbation of the temperature due to the end plug levels out very fast, and it has been verified that only the particular integral of (1) contributes to thermal stresses.

(+) Manuscript received on May 12, 1967.

(++) Axial TEmperature And Stress distribution

The particular integral of (1) is given by the following convolution integral (see appendix 1)

$$T(x) = \frac{m}{2h} \int_{-\infty}^{+\infty} q(y) e^{-m|x-y|} dy \quad (3)$$

It is obvious that the contribution to the temperature at a place x of a flux at a place y levels out with increasing $|x-y|$ and the integral can be truncated at an appropriate value of $|x-y|$.

For later convenience the following abbreviations are introduced:

$$QM = \int_{-\infty}^x q(y) e^{-m(x-y)} dy \quad (4)$$

$$QP = \int_x^{\infty} q(y) e^{-m(y-x)} dy \quad (5)$$

Equation (3) can now be written as:

$$T = \frac{m}{2h} (QM + QP) \quad (6)$$

The integrals QM and QP can in some cases be calculated analytically. The purpose of this paper, however, is rather to develop a numerical method to handle empirical neutron flux distributions. In chapter 5 is explained, how by defining the flux level at discrete points x_i the temperature at any point x can be computed from equation (6).

3. THERMAL STRESSES FOR A GIVEN TEMPERATURE DISTRIBUTION

In the classical theory for symmetrical loaded thin cylinders, the analogy of the elastic embedded beam is employed. This theory, which is given in handbooks on the subject (ref. 1 and 2), is repeated in appendix 2, including the correction for the temperature field and an approximate theory for finned cannings. It turns out that for finned cannings the differential equation governing the radial displacement of the canning wall is the same as for smooth cannings.

$$\frac{d^4 u}{dx^4} + 4 \beta^4 u = 4 \beta^4 \alpha a T \quad (1)$$

The homogeneous solution of this equation is dealt with in detail in handbooks on the subject (ref. 1 and 2). It can be written as:

$$u(x) = e^{-\beta x}(A \sin \beta x + B \cos \beta x) + e^{\beta x}(C \sin \beta x + D \cos \beta x) \quad (2)$$

As can be seen from (2), it is only related with boundary effects. The thermal stress problem due to axial temperature variations consists therefore rather in finding a particular integral of (1), taking care of the right-hand-side member. Eventually an homogeneous solution at the ends has to be added to satisfy the boundary conditions.

The particular integral of equation (1) is given by the convolution integral (see appendix 3):

$$u(x) = \alpha a T(x) + \frac{\alpha a}{4\beta} \int_{-\infty}^{+\infty} \frac{d^2 T(y)}{dy^2} \psi \left\{ \beta |x - y| \right\} dy \quad (3)$$

$$\psi(\beta x) = e^{-\beta x} (\cos \beta x - \sin \beta x)$$

From the displacement field, the moment M, the shear force Q and the hoop force H are found by differentiating (see appendix 2).

For convenience the following abbreviations are introduced:

$$\text{TCM} = \int_{-\infty}^x \frac{d^2 T(y)}{dy^2} e^{-\beta(x-y)} \cos \beta(x-y) dy \quad (4)$$

$$\text{TCP} = \int_x^{\infty} \frac{d^2 T(y)}{dy^2} e^{-\beta(y-x)} \cos \beta(y-x) dy \quad (5)$$

$$\text{TSM} = \int_{-\infty}^x \frac{d^2 T(y)}{dy^2} e^{-\beta(x-y)} \sin \beta(x-y) dy \quad (6)$$

$$\text{TSP} = \int_x^{\infty} \frac{d^2 T(y)}{dy^2} e^{-\beta(y-x)} \sin \beta(y-x) dy \quad (7)$$

Furthermore, in order to facilitate the algebra, complex functions are introduced:

$$\begin{aligned} \psi(\beta x) &= e^{-\beta x} (\cos \beta x - \sin \beta x) \\ &= (\text{Re} - \text{Im}) e^{-\beta x(1-j)} \end{aligned} \quad (8)$$

$$\begin{aligned} \varphi(\beta x) &= e^{-\beta x} (\cos \beta x + \sin \beta x) \\ &= (\text{Re} + \text{Im}) e^{-\beta x(1-j)} \end{aligned} \quad (9)$$

$$\text{TM} = \text{TCM} + j\text{TSM} \quad (10)$$

$$\text{TP} = \text{TCP} + j\text{TSP} \quad (11)$$

The displacement field (3) can then be written as:

$$u = \alpha a T + \frac{\alpha a}{4\beta} (\text{TCM} + \text{TCP} - \text{TSM} - \text{TSP}) \quad (12)$$

The derivatives become:

$$\frac{du}{dx} = \alpha a \frac{dT}{dx} - \frac{1}{2} \alpha a (\text{TCM} - \text{TCP}) \quad (13)$$

$$\frac{d^2u}{dx^2} = \frac{1}{2} \alpha a \beta (TCM + TCP + TSM + TSP) \quad (14)$$

$$\frac{d^3u}{dx^3} = -\alpha a \beta^2 (TSM - TSP) \quad (15)$$

$$\frac{d^4u}{dx^4} = -\alpha a \beta^3 (TCM + TCP - TSM - TSP) \quad (16)$$

In chapter 5 is explained how by defining the temperature at discrete points x_i , the integrals TCM, TCP, ...etc. can be computed for any value of x .

4. THERMAL STRESSES FOR GIVEN FLUX DISTRIBUTION

The relations derived in chapter 2 and 3 are combined. The displacement field is now given by the following convolution integral (see appendix 3):

$$\begin{aligned} u(x) = & \frac{\alpha a m}{2h} \int_{-\infty}^{+\infty} q(y) e^{-m|x-y|} dy \\ & - \frac{\alpha a m^2}{4\beta h} \frac{1}{1+4 \left(\frac{\beta}{m}\right)^4} \left\{ 4 \left(\frac{\beta}{m}\right)^4 \int_{-\infty}^{+\infty} q(y) \psi(\beta|x-y|) dy \right. \\ & \quad - 2 \left(\frac{\beta}{m}\right)^2 \int_{-\infty}^{+\infty} q(y) \phi(\beta|x-y|) dy \\ & \quad \left. + 2 \left(\frac{\beta}{m}\right) \int_{-\infty}^{+\infty} q(y) e^{-m|x-y|} dy \right\} \quad (1) \end{aligned}$$

For convenience the following abbreviations are introduced:

$$MQM = \int_{-\infty}^x q(y) e^{-m(x-y)} dy \quad (2)$$

$$MQP = \int_x^{\infty} q(y) e^{-m(y-x)} dy \quad (3)$$

$$QCM = \int_{-\infty}^x q(y) e^{-\beta(x-y)} \cos \beta(x-y) dy \quad (4)$$

$$QCP = \int_x^{\infty} q(y) e^{-\beta(y-x)} \cos \beta(y-x) dy \quad (5)$$

$$QSM = \int_{-\infty}^x q(y) e^{-\beta(x-y)} \sin \beta (x-y) dy \quad (6)$$

$$QSP = \int_x^{\infty} q(y) e^{-\beta(y-x)} \sin \beta (y-x) dy \quad (7)$$

The displacement field can then be written as:

$$\begin{aligned} u &= \frac{\alpha am}{2h} (MQM + MQP) \\ &- \frac{\alpha am^2}{4\beta h} \frac{1}{1+4\left(\frac{\beta}{m}\right)^4} \left[4\left(\frac{\beta}{m}\right)^4 (QCM + QCP - QSM - QSP) \right. \\ &\quad \left. - 2\left(\frac{\beta}{m}\right)^2 (QCM + QCP + QSM + QSP) \right. \\ &\quad \left. + 2\left(\frac{\beta}{m}\right) (MQM + MQP) \right] \end{aligned} \quad (8)$$

The derivatives become:

$$\begin{aligned} \frac{du}{dx} &= -\frac{\alpha am^2}{2h} (MQM - MQP) \\ &+ \frac{\alpha am^2}{2h} \frac{1}{1+4\left(\frac{\beta}{m}\right)^4} \left[4\left(\frac{\beta}{m}\right)^4 (QCM - QCP) \right. \\ &\quad \left. - 2\left(\frac{\beta}{m}\right)^2 (QSM - QSP) \right. \\ &\quad \left. + (MQM - MQP) \right] \end{aligned} \quad (9)$$

$$\begin{aligned} \frac{d^2u}{dx^2} &= \frac{\alpha am^3}{2h} (MQM + MQP) \\ &- \frac{\alpha am^2}{2h} \frac{\beta}{1+4\left(\frac{\beta}{m}\right)^4} \left[4\left(\frac{\beta}{m}\right)^4 (QCM + QSM + QCP + QSP) \right. \\ &\quad \left. + 2\left(\frac{\beta}{m}\right)^2 (QCM + QCP - QSM - QSP) \right. \\ &\quad \left. + \left(\frac{m}{\beta}\right) (MQM + MQP) \right] \end{aligned} \quad (10)$$

$$\begin{aligned}
\frac{d^3u}{dx^3} = & -\frac{\alpha am^4}{2h} \quad (\text{MQM} - \text{MQP}) \\
& + \frac{\alpha am^2}{2h} \frac{2\beta^2}{1+4\left(\frac{\beta}{m}\right)^4} \left[4\left(\frac{\beta}{m}\right)^4 (\text{QSM} - \text{QSP}) \right. \\
& \quad \quad \quad + 2\left(\frac{\beta}{m}\right)^2 (\text{QCM} - \text{QCP}) \\
& \quad \quad \quad \left. - \frac{1}{2}\left(\frac{m}{\beta}\right)^2 (\text{MQM} - \text{MQP}) \right]
\end{aligned} \tag{11}$$

$$\begin{aligned}
\frac{d^4u}{dx^4} = & \frac{\alpha am^5}{2h} \quad (\text{MQM} + \text{MQP}) \\
& + \frac{\alpha am^2}{2h} \frac{2\beta^3}{1+4\left(\frac{\beta}{m}\right)^4} \left[4\left(\frac{\beta}{m}\right)^4 (\text{QCM} + \text{QCP} - \text{QSM} - \text{QSP}) \right. \\
& \quad \quad \quad - 2\left(\frac{\beta}{m}\right)^2 (\text{QCM} + \text{QSM} + \text{QCP} + \text{QSP}) \\
& \quad \quad \quad \left. - \frac{1}{2}\left(\frac{m}{\beta}\right)^3 (\text{MQM} + \text{MQP}) \right]
\end{aligned} \tag{12}$$

In chapter 5 is explained how by defining the flux level at discrete points x_i the integrals QCM, QCP etc. can be computed for any value of x .

5. NUMERICAL METHODS

As shown in the previous chapters the determination of the temperature and thermal stress distribution can be reduced to the evaluation of the convolution integrals of the type:

$$I(y) = \int_{-\infty}^{+\infty} q(x) e^{-\beta|x-y|} \cos\beta|x-y| dx \tag{1}$$

This kind of integrals can be evaluated analytically for a lot of functions, but the actual determination of the maximum stress and the place where it occurs remains a laborious algebraic computation.

It proved to be worthwhile to automatize this kind of computations by means of a digital computer, enabling also to work directly with empirical flux distributions.

Consider for that a flux distribution defined in N discrete points:

$$\begin{aligned} (x_i, q_i) \quad & i = 1 \rightarrow N \\ & x_i < x_{i+1} \end{aligned} \quad (2)$$

Assuming a linear distribution of the flux between two adjacent points, the function q is then represented by:

$$\begin{aligned} q(x) &= A_i + B_i x \\ B_i &= \frac{q_{i+1} - q_i}{x_{i+1} - x_i} \\ A_i &= q_i - B_i x_i \end{aligned} \quad (3)$$

The flux level for $x < x_1$ and $x > x_N$ is taken equal to q_1 respectively q_N : Their contribution to the thermal stress at points between x_1 and x_N decreases very rapidly with the distance to x_1 respectively x_N .

For $x_M < y < x_{M+1}$ the integral QCM, for example, can then be written as:

$$\begin{aligned} \text{QCM} &= \int_{-\infty}^{x_1} q_1 e^{-\beta(y-x)} \cos\beta(y-x) dx \\ &+ \sum_{i=1}^{M-1} \int_{x_i}^{x_{i+1}} (A_i + B_i x) e^{-\beta(y-x)} \cos\beta(y-x) dx \\ &+ \int_{x_M}^y (A_M + B_M x) e^{-\beta(y-x)} \cos\beta(y-x) dx \end{aligned} \quad (4)$$

These integrals can be evaluated analytically, by partial integration or by introducing complex functions as in chapter 3. Introducing the abbreviations:

$$\begin{aligned} \text{FC}(x) &= e^{-\beta x} \cos \beta x \\ \text{FS}(x) &= e^{-\beta x} \sin \beta x \\ \text{F}(x) &= e^{-mx} \end{aligned} \quad (5)$$

the following expressions are obtained:

$$\begin{aligned} \text{QCM} &= \frac{1}{2\beta} A_0 \{ \text{FC}(y-x_1) - \text{FS}(y-x_1) \} \\ &+ \frac{1}{2\beta} \sum_{i=1}^{M-1} (A_i + B_i x_{i+1}) \{ \text{FC}(y-x_{i+1}) - \text{FS}(y-x_{i+1}) \} \\ &- \frac{1}{2\beta} \sum_{i=1}^{M-1} (A_i + B_i x_i) \{ \text{FC}(y-x_i) - \text{FS}(y-x_i) \} \\ &+ \frac{1}{2\beta^2} \sum_{i=1}^{M-1} B_i \{ \text{FS}(y-x_{i+1}) - \text{FS}(y-x_i) \} \\ &+ \frac{1}{2\beta} (A_M + B_M y) \\ &- \frac{1}{2\beta} (A_M + B_M x_M) \{ \text{FC}(y-x_M) - \text{FS}(y-x_M) \} \\ &- \frac{1}{2\beta^2} B_M \text{FS}(y-x_M) \end{aligned} \quad (6)$$

$$\begin{aligned} \text{QSM} &= \frac{1}{2\beta} A_0 \{ \text{FC}(y-x_1) + \text{FS}(y-x_1) \} \\ &+ \frac{1}{2\beta} \sum_{i=1}^{M-1} (A_i + B_i x_{i+1}) \{ \text{FC}(y-x_{i+1}) + \text{FS}(y-x_{i+1}) \} \\ &- \frac{1}{2\beta} \sum_{i=1}^{M-1} (A_i + B_i x_i) \{ \text{FC}(y-x_i) + \text{FS}(y-x_i) \} \\ &- \frac{1}{2\beta^2} \sum_{i=1}^{M-1} B_i \{ \text{FC}(y-x_{i+1}) - \text{FC}(y-x_i) \} \\ &+ \frac{1}{2\beta} (A_M + B_M y) \\ &- \frac{1}{2\beta} (A_M + B_M x_M) \{ \text{FC}(y-x_M) + \text{FS}(y-x_M) \} \\ &- \frac{1}{2\beta^2} B_M \{ 1 - \text{FC}(y-x_M) \} \end{aligned} \quad (7)$$

$$\begin{aligned}
\text{QCP} = & -\frac{1}{2\beta} (A_M + B_M x_{M+1}) \{ \text{FC}(x_{M+1} - y) - \text{FS}(x_{M+1} - y) \} \\
& + \frac{1}{2\beta} (A_M + B_M y) \\
& + \frac{1}{2\beta^2} B_M \text{FS}(x_{M+1} - y) \\
& - \frac{1}{2\beta} \sum_{i=M+1}^{N-1} (A_i + B_i x_{i+1}) \{ \text{FC}(x_{i+1} - y) - \text{FS}(x_{i+1} - y) \} \quad (8) \\
& + \frac{1}{2\beta} \sum_{i=M+1}^{N-1} (A_i + B_i x_i) \{ \text{FC}(x_i - y) - \text{FS}(x_i - y) \} \\
& + \frac{1}{2\beta^2} \sum_{i=M+1}^{N-1} B_i \{ \text{FS}(x_{i+1} - y) - \text{FS}(x_i - y) \} \\
& + \frac{1}{2\beta} A_N \{ \text{FC}(x_N - y) - \text{FS}(x_N - y) \}
\end{aligned}$$

$$\begin{aligned}
\text{QSP} = & -\frac{1}{2\beta} (A_M + B_M x_{M+1}) \{ \text{FC}(x_{M+1} - y) + \text{FS}(x_{M+1} - y) \} \\
& + \frac{1}{2\beta} (A_M + B_M y) \\
& - \frac{B_M}{2\beta^2} \{ \text{FC}(x_{M+1} - y) - 1 \} \\
& - \frac{1}{2\beta} \sum_{i=M+1}^{N-1} (A_i + B_i x_{i+1}) \{ \text{FC}(x_{i+1} - y) + \text{FS}(x_{i+1} - y) \} \quad (9) \\
& + \frac{1}{2\beta} \sum_{i=M+1}^{N-1} (A_i + B_i x_i) \{ \text{FC}(x_i - y) + \text{FS}(x_i - y) \} \\
& - \frac{1}{2\beta^2} \sum_{i=M+1}^{N-1} B_i \{ \text{FC}(x_{i+1} - y) - \text{FC}(x_i - y) \} \\
& + \frac{1}{2\beta} A_N \{ \text{FC}(x_N - y) + \text{FS}(x_N - y) \}
\end{aligned}$$

$$\begin{aligned}
MQM = & \frac{1}{m} A_0 F(y - x_1) \\
& + \frac{1}{m} \sum_{i=1}^{M-1} (A_i + B_i x_{i+1}) F(y - x_{i+1}) \\
& - \frac{1}{m} \sum_{i=1}^{M-1} (A_i + B_i x_i) F(y - x_i) \\
& - \frac{1}{m^2} \sum_{i=1}^{M-1} B_i (F(y - x_{i+1}) - F(y - x_i)) \\
& + \frac{1}{m} (A_M + B_M y) \\
& - \frac{1}{m} (A_M + B_M x_M) F(y - x_M) \\
& - \frac{1}{m^2} B_M (1 - F(y - x_M))
\end{aligned} \tag{10}$$

$$\begin{aligned}
MQP = & - \frac{1}{m} (A_M + B_M x_{M+1}) F(x_{M+1} - y) \\
& + \frac{1}{m} (A_M + B_M y) \\
& - \frac{1}{m^2} B_M (F(x_{M+1} - y) - 1) \\
& - \frac{1}{m} \sum_{i=M+1}^{N-1} (A_i + B_i x_{i+1}) F(x_{i+1} - y) \\
& + \frac{1}{m} \sum_{i=M+1}^{N-1} (A_i + B_i x_i) F(x_i - y) \\
& - \frac{1}{m^2} \sum_{i=M+1}^{N-1} B_i (F(x_{i+1} - y) - F(x_i - y)) \\
& + \frac{1}{m} A_N F(x_N - y)
\end{aligned} \tag{11}$$

The value of M is defined by $x_M \leq y < x_{M+1}$

In cases where the temperature distribution is known from measurements, the equations derived in chapter 3 are to be used.

Consider for this a temperature distribution defined in N discrete points :

$$(x_i, T_i) \quad i = 1 \rightarrow N \quad x_i < x_{i+1} \quad (12)$$

Assuming a linear temperature distribution between two adjacent points x_i and x_{i+1} , the change in gradient at a point x_i is defined by

$$D2T_i = \frac{T_{i+1} - T_i}{x_{i+1} - x_i} - \frac{T_i - T_{i-1}}{x_i - x_{i-1}} \quad (13)$$

The integrals TCM, TCP etc. as defined in chapter 3 become:

$$TCM = \sum_{i=1}^M D2T_i \quad FC (y - x_i) \quad (14)$$

$$TCP = \sum_{i=M+1}^N D2T_i \quad FC (x_i - y) \quad (15)$$

$$FSM = \sum_{i=1}^M D2T_i \quad FS (y - x_i) \quad (16)$$

$$TSP = \sum_{i=M+1}^N D2T_i \quad FS (x_i - y) \quad (17)$$

M is defined by $x_M < y < x_{M+1}$

Equations (6), (7).....(11) and (14), (15), (16) and (17) are the basic equations of the code ATEAS.

6. NUMERICAL APPLICATION TO A G 19 FINNED CANNING

In fig. 10 is given an enlarged photograph of the cross-section of a G 19 finned canning. Comparison with Fig. 6 yields the following values of the dimensions of the fin:

$$\begin{array}{ll} e_1 = 0.094 \text{ cm} & b_1 = 0.042 \text{ cm} \\ e_2 = 0.194 \text{ cm} & b_2 = 0.025 \text{ cm} \\ a = 0.78 \text{ cm} & b_3 = 0.038 \text{ cm} \end{array}$$

From these values ATEAS determined the parameters m and β

$$\begin{aligned}\beta &= 3.34 \text{ cm}^{-1} \\ m &= 2.611 \text{ cm}^{-1} \quad (h = 1 \text{ Watt/cm}^2 \text{ } ^\circ\text{C}, \lambda = 1.8 \text{ Watt/cm } ^\circ\text{C}) \\ m &= 3.692 \text{ cm}^{-1} \quad (h = 2 \text{ Watt/cm}^2 \text{ } ^\circ\text{C}, \lambda = 1.8 \text{ Watt/cm } ^\circ\text{C})\end{aligned}$$

The flux distributions are chosen as given in Fig. 11:

Nominal value: $q = 135 \text{ Watt/cm}^2$ on finned surface
Flux peak varying from 0% up to 50% over a length of 6 cm.

The corresponding temperature distributions, as calculated by ATEAS, are given in Fig. 11, respectively for $h = 1$ and $h = 2 \text{ Watt/cm}^2 \text{ } ^\circ\text{C}$, and for the various flux peaks as mentioned before.

In Fig. 12 the temperature distribution for $h = 1 \text{ Watt/cm}^2 \text{ } ^\circ\text{C}$ is repeated on a larger scale. The bending stresses respectively at the top of the fin and at the inner canning wall, calculated for a Young's modulus $E = 400,000 \text{ kg/cm}^2$, are also represented in Fig. 12.

In Fig. 13, the curves of Fig. 12 are repeated for the case of $h = 2 \text{ Watt/cm}^2 \text{ } ^\circ\text{C}$.

It is noted that the stresses are proportional to the nominal value of the flux and also to Young's modulus, and can therefore easily be determined for other values of nominal flux and Young's modulus.

The equivalent stress at the corner of the fin, calculated according to the Huber deformation energy criterion, is small as compared to the bending stress (see Fig. 14). It can therefore be ignored in the design philosophy. This confirms that the deformation due to shear stresses is small as compared to the deformation due to bending stresses, which is one of the assumptions of the theory.

As can be seen from figures 12 and 13, the thermal bending stress phenomenon due to axial temperature variations is a local one, and it does not influence eventual bending stresses at the weld of canning to end plug, if the distance between fuel pellets and weld is bigger than about 1 cm (for G 19).

It might be of interest to compare the refined theory for finned cannings with the one for smooth cannings, and to try to determine an equivalent canning wall thickness for the homogenized finned canning. It will be shown that different equivalent thicknesses are to be applied for the temperature and for the stress calculation.

For $h = 1 \text{ Watt/cm}^2 \text{ } ^\circ\text{C}$ the parameter m for G 19 was equal to

$$m = 2.611 \text{ cm}^{-1}$$

According to equation (1) of appendix 1 the equivalent thickness for an homogenized G 19 canning becomes

$$e = \frac{h}{\lambda m^2} = 0.0815 \text{ cm.}$$

It turns out that the equivalent thickness is about 12% lower than the cylinder wall thickness of the finned canning ($e_1 = 0.094 \text{ cm}$). Physically it means that the additional surface (wetted periphery) introduced by the fin has a greater influence on the axial conduction process than the additional cross-section, a phenomenon which verifies itself also for radial conduction.

As concerns the stress calculation, an equivalent thickness can be computed from equation (8) of appendix 2, in such a way that the elastic wave length is the same:

$$e = \sqrt{\frac{3(1 - \nu^2)}{a \beta^2}} = 0.1892 \text{ cm}$$

$$(\beta = 3.34 \text{ cm}^{-1})$$

This equivalent thickness is about 2% lower than the height of the fins ($e_2 = 0.194$). This is accidental and cannot be taken as a general law. The wave length β is determined by the ratio of the circumferential rigidity (tension) to the axial rigidity (bending), both per unit length (equation 8, appendix 2). To obtain for the same wave length equal stresses, an equivalent thickness should be introduced such that the distances from neutral grain to grain of maximum bending stress

are equal:

$$e = 2 (e_2 - h_n)$$

For a G 19 canning $h_n = 0.0785$ cm

$$e = 0.231 \text{ cm.}$$

This equivalent thickness is about 20% higher than the height of the fins.

Summarizing, it seems not to be possible to homogenize a finned canning by introducing a kind of average thickness, but m , β and h_n are to be determined from the formulae of appendices 1 and 2.

7. CONCLUSION AND FINAL REMARKS

A theory has been developed to determine the temperature and thermal stress distribution due to axial flux variations for smooth and for finned cannings, assuming a linear stress-strain relation (Hook's law). The digital code ATEAS handles either empirical flux distributions or empirical temperature distributions. The latter is of interest for cases where the temperature distribution is calculated by taking into account the contribution of the fuel in the axial conduction (see ref. 3), which is neglected in this paper.

From the numerical example of chapter 6 follows that the phenomenon is local, and stresses vanish at about 1 cm distance of the flux perturbation (G 19).

For a G 19 finned canning with

nominal flux	$q = 135 \text{ Watt/cm}^2$
peak	20 %
heat transfer	$h = 2 \text{ Watt/cm}^2 \text{ } ^\circ\text{C}$
Young's Modulus	$E = 4000 \text{ kg/mm}^2$
	(450°C)

the maximum bending stress at the top of the fin is equal

to

$$\sigma = 1.1 \text{ kg/mm}^2$$

Shear stresses can be neglected in the design philosophy.

If, like in other than G 19 ORGEL type of cannings, spacer fins are present, it is recommended to cut them in regions of accentuated temperature variations, in order to prevent excessive bending stresses at their outer grains.

ACKNOWLEDGEMENT

ATEAS has been written by Mr. R. Meelhuysen. His accurate way of programming is very acknowledged and has been of major importance for the realisation of ATEAS.

R E F E R E N C E S

=====

1. C.B. BIEZENO, R. GRAMMEL
"Technische Dynamik"
Band 1, Springer Verlag (1939), Berlin - Goettingen Heidelberg

2. S. TIMOSHENKO
"Theory of Plates and Shells"
United Engineering Trustees, Inc. (1940)

3. E. ARANOVITCH, E. LABARRE, J. REYNEN
"Etudes des perturbations circonférentielles et axiales
de température dans une gaine cylindrique d'élément
combustible (Méthodes mathématique et rhéoanalogique)"
EUR 2480 f (1965)

N O M E N C L A T U R E

=====

a	radius of canning
A_i	constants in flux functions
A	integration constant
b	width
b_1) dimensions defining the finned
b_2	(canning wall cross-section
b_3)
B_i	constant in flux functions
e	wall thickness of smooth canning
e_1	wall thickness of finned canning
e_2	height of fin
h	heat transfer coefficient
h_n	coordinate of neutral grain
i	index indicating axial position
j	$\sqrt{-1}$
m	thermal wave length
p	pressure
q	flux
Q	Fourier transform of flux
s	Fourier coordinate
S	cross-section of finned canning wall
t	imaginary coordinate in z plane
T	temperature
u	radial displacement
U	Fourier transform of radial displacement
x	axial coordinate
y	auxiliary axial coordinate
z	complex coordinate
α	linear thermal dilatation coefficient
β	elastic wave length
ξ	auxiliary axial coordinate
θ	Fourier transform of temperature
λ	conductivity of canning

DIFFERENTIAL EQUATION GOVERNING THE AXIAL TEMPERATURE
DISTRIBUTION AND ITS SOLUTION

A. Canning without fins

A heat balance in axial direction yields (see Fig. 1):

$$-\lambda e \frac{d^2 T}{dx^2} = q - h T \quad (1)$$

with $m = \sqrt{\frac{h}{\lambda e}}$ one obtains

$$\frac{d^2 T}{dx^2} - m^2 T = -\frac{m^2}{h} q \quad (2)$$

B. Canning with fins

Consider the cross section as given in Fig. 2.

$$-\lambda S \frac{d^2 T}{dx^2} = 2q(b_1 + b_2 + b_3) - 2h \left(b_1 + b_3 + \sqrt{b_2^2 + (e_2 - e_1)^2} \right) \quad (3)$$

with

$$m = \sqrt{\frac{h}{\lambda} \frac{b_1 + b_3 + \sqrt{b_2^2 + (e_2 - e_1)^2}}{b_1 e_1 + b_3 e_2 + \frac{1}{2} b_2 (e_2 + e_1)}} \quad (4)$$

and

$$FC = \frac{b_1 + b_3 + \sqrt{b_2^2 + (e_2 - e_1)^2}}{b_1 + b_2 + b_3} \quad (5)$$

one obtains:

$$\frac{d^2 T}{dx^2} - m^2 T = -\frac{m^2}{h} \left(\frac{q}{FC} \right) \quad (6)$$

Equation (6) is similar to equation (2), if for finned cannings the flux is divided by the finning coefficient FC.

C. Solution of the heat transport equation

The Fourier transforms of T and q are defined by:

$$\theta(s) = \frac{1}{\sqrt{2\pi}} \int_{-\infty}^{+\infty} T(x) e^{jsx} dx \quad (7)$$

$$Q(s) = \frac{1}{\sqrt{2\pi}} \int_{-\infty}^{+\infty} q(x) e^{jsx} dx \quad (8)$$

The inverse transforms are defined by:

$$T(x) = \frac{1}{\sqrt{2\pi}} \int_{-\infty}^{+\infty} \theta(s) e^{-jsx} ds \quad (9)$$

$$q(x) = \frac{1}{\sqrt{2\pi}} \int_{-\infty}^{+\infty} Q(s) e^{-jsx} ds \quad (10)$$

If $f_1(s)$ and $f_2(s)$ represent respectively the Fourier transform of the functions $F_1(x)$ and $F_2(x)$, then the convolution integral of F_1 and F_2 is defined by:

$$\begin{aligned} \int_{-\infty}^{+\infty} F_1(\xi) F_2(x-\xi) d\xi &= \int_{-\infty}^{+\infty} F_1(x-\xi) F_2(\xi) d\xi = \\ &= \int_{-\infty}^{+\infty} f_1(s) f_2(s) e^{-jsx} ds \end{aligned} \quad (11)$$

Inserting the transforms into the differential equation (2) yields:

$$\theta = \frac{m^2}{h} \frac{Q}{s^2 + m^2} \quad (12)$$

Applying the inverse transform gives:

$$T(x) = \frac{1}{\sqrt{2\pi}} \frac{m^2}{h} \int_{-\infty}^{+\infty} \frac{Q(s) e^{-jsx}}{s^2 + m^2} ds \quad (13)$$

Comparing (13) with (11) and calling $Q(s) = f_1(s)$ and $\frac{1}{s^2+m^2} = f_2(s)$, equation(13) becomes:

$$T(x) = \frac{1}{\sqrt{2\pi}} \frac{m^2}{h} \int_{-\infty}^{+\infty} q(\xi) F_2(x-\xi) d\xi \quad (14)$$

The function $F_2(x)$ is defined from the inverse of $f_2(s)$

$$F_2(x) = \frac{1}{\sqrt{2\pi}} \int_{-\infty}^{+\infty} \frac{e^{-jsx}}{s^2+m^2} ds \quad (15)$$

The latter integral is calculated by contour integration. Suppose x positive and consider the contour as presented in Fig. 3. For $R \rightarrow \infty$ the integrand becomes zero at the circle:

$$\oint_{R \rightarrow \infty} \frac{e^{-jzx}}{z^2 + m^2} dz = \int_{+\infty}^{-\infty} \frac{e^{-jsx}}{s^2 + m^2} ds \quad (16)$$

The poles of the integrand are at $z = \pm jm$ and it is observed that only the pole $z = -jm$ is inside the contour. The residue at the pole $z = -jm$ becomes

$$\text{residue} = \frac{e^{-mx}}{-2jm} \quad (17)$$

$$\begin{aligned} \int_{+\infty}^{-\infty} \frac{e^{-jsx}}{s^2 + m^2} ds &= 2\pi j \Sigma \text{ residue's} \\ &= 2\pi \left(\frac{e^{-mx}}{-2m} \right) \end{aligned} \quad (18)$$

Finally, still for positive x , one gets

$$F_2(x) = \sqrt{2\pi} \frac{e^{-mx}}{2m} \quad (19)$$

For physical reasons it is obvious that F_2 should be an even function and therefore:

$$F_2(x) = \sqrt{2\pi} \frac{e^{-m|x|}}{2m} \quad (20)$$

The temperature is then given by the following convolution integral:

$$T(x) = \frac{m}{2h} \int_{-\infty}^{+\infty} q(\xi) e^{-m|x-\xi|} d\xi \quad (21)$$

THE DIFFERENTIAL EQUATION GOVERNING THE DISPLACEMENT
OF A THIN CYLINDER WITH SYMMETRICAL LOADING

In order to derive a correction for finned cannings, the classical theory as presented in handbooks on the subject (ref. 1 and 2) is repeated.

A. Canning without fins

Consider an elementary part of the cylinder as depicted in Fig. 4. Due to symmetry its displacement is only in radial direction and denoted by u , positive when the radius tends to become bigger. The elementary part is regarded as a cantilever, loaded by forces and moments as given in Fig. 4. Deformations due to the shear force are neglected, which is by the way usual for cantilevers which are not high as compared to their length.

Application of the elementary bending theory yields:

$$\frac{E e^3}{12} \frac{d^2 u}{dx^2} = M_{x\phi} - \gamma M_{\phi x} \quad (1)$$

$$\frac{E e^3}{12} \left(\frac{1}{a} - \frac{1}{a+u} \right) = -\gamma M_{x\phi} + M_{\phi x}$$

The change in curvature in tangential direction is small of the second order:

$$\frac{1}{a} - \frac{1}{a+u} \approx \frac{u}{a^2} \approx 0 \quad (2)$$

Equations (1) become:

$$M_{\phi x} = \gamma M_{x\phi} \quad (3)$$

$$\frac{E e^3}{12} \frac{d^2 u}{dx^2} = (1 - \gamma^2) M_{x\phi}$$

The hoop force H is related to the displacement by

$$H = E e \left(\frac{u}{a} - \alpha T \right) \quad (4)$$

Equations (3) and (4) are the stress-displacement relations of the problem.

The equilibrium equations follow from Fig. 4.

$$\frac{dQ}{dx} = -p + \frac{H}{a} \quad (5)$$

$$\frac{dM}{dx} = -Q \quad (6)$$

Combination of (3), (4), (5) and (6) yields:

$$\frac{d^4 u}{dx^4} + 4\beta^4 u = 4\beta^4 \left(\alpha a T + \frac{pa^2}{E} \right) \quad (7)$$

$$4\beta^4 = \frac{12(1-\nu^2)}{a^2 e^2} \quad (8)$$

B. Canning with fins

Consider the elementary part as given in Fig. 5. As compared to Fig. 4, the equilibrium equations are not changed. Only the relations between the displacement u and the forces and moments have to be changed.

As regards bending in axial direction, the inertia moment of the complicated cross-section (Fig 6) should be introduced. As in elementary bending theory a linear stress distribution can be assumed.

As regards bending in tangential direction (Fig. 7) the contribution of the fin is more difficult to calculate. In the canning without fin, the anti-elastical bending in tangential direction causes an increase of rigidity in axial direction of about 10% $\left(\frac{1}{1-\nu^2} - 1 \approx 0.1 \right)$. It is therefore less important to know the exact elasticity in tangential direction. An easy way to estimate it, is to assume a linear stress distribution in every cross-section in φ direction.

The hoop force H causes a displacement u , which can be calculated by assuming an uniform stress distribution in every cross-section in φ direction (Fig. 8).

Adopting the above mentioned hypothesis yields:

$$\frac{d^2 u}{dx^2} = \frac{M_{x\varphi}}{E I_{x\varphi}} - \gamma \frac{M_{\varphi x}}{E I_{\varphi x}} \quad (9)$$

$$\frac{1}{a} - \frac{1}{a+u} = \frac{-\gamma M_{x\varphi}}{E I_{x\varphi}} + \frac{M_{\varphi x}}{E I_{\varphi x}} \approx 0 \quad (10)$$

$$M_{\varphi x} = \gamma \frac{I_{\varphi x}}{I_{x\varphi}} M_{x\varphi} \quad (11)$$

$$\frac{d^2 u}{dx^2} = \frac{(1-\gamma^2) M_{x\varphi}}{E I_{x\varphi}} \quad (12)$$

$$I_{x\varphi} = \iint (z-h_n)^2 dA \quad (\text{see Fig. 6})$$

$$h_n = \frac{\iint z dA}{\iint dA} \quad (\text{see Fig. 6}) \quad (13)$$

$$I_{x\varphi} = \frac{1}{3(b_1+b_2+b_3)} \left[b_1 \left((e_1-h_n)^3 + h_n^3 \right) + b_3 \left((e_2-h_n)^3 + h_n^3 \right) + b_2 \left(\left((e_2-h_n)^2 + (e_1-h_n)^2 \right) \left(\frac{e_1 + e_2 - 2h_n}{4} + h_n^3 \right) \right) \right] \quad (14)$$

$$h_n = \frac{1}{2} \frac{b_1 e_1^2 + b_3 e_2^2 + \frac{1}{3} b_2 (e_1^2 + e_1 e_2 + e_2^2)}{b_1 e_1 + \frac{1}{2} b_2 (e_1 + e_2) + b_3 e_2} \quad (15)$$

$$I_{\varphi x} = \frac{b_1+b_2+b_3}{12 \int \frac{db}{e^3}} \quad (\text{see Fig. 7}) \quad (16)$$

$$I_{\phi x} = \frac{b_1 + b_2 + b_3}{12 \left(\frac{b_1}{e_1^3} + \frac{b_2(e_1 + e_2)}{2e_1^2 e_2^2} + \frac{b_3}{e_2^2} \right)} \quad (17)$$

$$H = E \left(\frac{u}{a} - \alpha T \right) h_1 \quad (18)$$

$$h_1 = \frac{b_1 + b_2 + b_3}{\int \frac{db}{e}} \quad (\text{see Fig. 8}) \quad (19)$$

$$h_1 = \frac{b_1 + b_2 + b_3}{\frac{b_1}{e_1} + \frac{b_2}{e_2 - e_1} \ln \frac{e_2}{e_1} + \frac{b_3}{e_2}} \quad (20)$$

The differential equation for the displacement becomes:

$$\frac{d^4 u}{dx^4} + 4 \beta^4 u = 4 \beta^4 \left(\alpha a T + \frac{pa^2}{Eh_1} \right) \quad (21)$$

$$4 \beta^4 = \frac{(1 - \nu^2) h_1}{I_{x\phi} a^2}$$

C. Stresses as function of the moments and forces

1. Canning without fins

Axial bending stress

$$\sigma_{bx} = \begin{array}{l} - \\ + \end{array} \frac{6 M_{x\phi}}{e^2} \quad \begin{array}{l} - \text{ outer wall} \\ + \text{ inner wall} \end{array} \quad (22)$$

Tangential bending stress

$$\sigma_{b\phi} = \begin{array}{l} - \\ + \end{array} \frac{6 \nu M_{x\phi}}{e^2} \quad \begin{array}{l} - \text{ outer wall} \\ + \text{ inner wall} \end{array} \quad (23)$$

Hoop stress

$$\sigma_{H\phi} = \frac{H}{e} \quad (24)$$

Shear stress in midplane

$$\tau_{x\phi} = \frac{3}{2} \frac{Q}{e} \quad \left(\begin{array}{l} \text{parabolic distribution} \\ \text{according to elementary} \\ \text{bending theory} \end{array} \right) \quad (25)$$

2. Canning with fins

Axial bending stress in outer grain of fin:

$$\sigma_{b,o,x} = - \frac{M}{I_{x\phi}} (e_2 - h_n) \quad (26)$$

Axial bending stress at interior canning wall:

$$\sigma_{b,i,x} = \frac{M}{I_{x\phi}} h_n \quad (27)$$

Tangential bending stress in cylinder wall:

$$\sigma_{b\phi} = \begin{array}{l} - \frac{6 M_{\phi x}}{e_1^2} \\ + \end{array} = \begin{array}{l} - \frac{\gamma I_{\phi x}}{I_{x\phi}} M_{x\phi} \\ + \end{array} \frac{6}{e_1^2} \quad (28)$$

- outer wall

+ inner wall

Tangential hoop stress

$$\sigma_{H,\phi} = \frac{H}{e_1} \quad (29)$$

It is noted that in the outer grain of the fin a maximum bending stress in axial direction occurs. In this grain no tangential bending stress exists. As other critical points should be mentioned the corner of the fin and the cylinder wall. The axial bending stress at that point is probably small:

$$\sigma = - E \frac{d^2 u}{dx^2} (e_1 - h_n) \quad (30)$$

The tangential bending stress (28) and the hoop stress (29) might be rather big. Besides an important shear stress occurs due to the varying bending moment in axial direction. As in elementary bending theory this

shear stress is calculated from the equilibrium equation in axial direction (see Fig. 9).

$$(b_2+b_3)\tau = - (b_1+b_2+b_3) \int_0^{e_1} \frac{d\sigma}{dx} d\xi \quad (31)$$

$$\tau_{x\varphi} = - \frac{b_1+b_2+b_3}{b_1+b_2} E \frac{d^3u}{dx^3} (h_n e_1 - \frac{1}{2} e_1^2) \quad (32)$$

According to the Huber rupture hypothesis the equivalent stress at the corner of the fin becomes:

$$\begin{aligned} \sigma_e &= \frac{1}{\sqrt{2}} \sqrt{(\sigma_1 - \sigma_2)^2 + (\sigma_2 - \sigma_3)^2 + (\sigma_3 - \sigma_1)^2} \\ &= \sqrt{(\sigma_1 + \sigma_2 + \sigma_3)^2 - 3(\sigma_1\sigma_2 + \sigma_2\sigma_3 + \sigma_3\sigma_1)} \end{aligned} \quad (33)$$

$$= \sqrt{(\sigma_x + \sigma_y + \sigma_z)^2 - 3(\sigma_x\sigma_y - \tau_{xy}^2 + \sigma_y\sigma_z - \tau_{yz}^2 + \sigma_z\sigma_x - \tau_{xz}^2)}$$

$$\sigma_e = \sqrt{(\sigma_a + \sigma_t + \sigma_H)^2 - 3\sigma_a(\sigma_t + \sigma_H) + 3\tau^2} \quad (34)$$

$$\sigma_a = \text{axial bending stress} \quad (30)$$

$$\sigma_t = \text{tangential bending stress} \quad (28)$$

$$\sigma_H = \text{tangential hoop stress} \quad (29)$$

$$\tau = \text{shear stress} \quad (32)$$

SOLUTION OF THE DIFFERENTIAL EQUATION GOVERNING
THE CYLINDER WALL DISPLACEMENT

1. Relation between displacement and temperature

The Fourier transform of the displacement field is defined by:

$$U(s) = \frac{1}{\sqrt{2\pi}} \int_{-\infty}^{+\infty} U(x) e^{jsx} dx \quad (1)$$

From the differential equation one obtains:

$$U(s) = 4\beta^4 \alpha a \frac{\theta}{s^4 + 4\beta^4} \quad (2)$$

(N.B. The pressure term is omitted for convenience, because it is usually constant in x direction. It is noted, that a varying pressure term can be treated in the same way as the temperature term).

Application of the inverse transform yields:

$$u(x) = 4\beta^4 \alpha a \frac{1}{\sqrt{2\pi}} \int_{-\infty}^{+\infty} \frac{\theta e^{-jsx}}{s^4 + 4\beta^4} ds \quad (3)$$

As in appendix 2 the integrand is regarded as the product of two functions $f_1(s)$ and $f_2(s)$, which are the transforms of two other functions $F_1(x)$ and $F_2(x)$.

$$u(x) = 4\beta^4 \alpha a \frac{1}{\sqrt{2\pi}} \int_{-\infty}^{+\infty} T(\xi) F_2(x-\xi) d\xi \quad (4)$$

$$F_2(x) = \frac{1}{\sqrt{2\pi}} \int_{-\infty}^{+\infty} \frac{e^{-jsx}}{s^4 + 4\beta^4} ds \quad (5)$$

The latter integral is evaluated by contour integration of the integral:

$$\oint \frac{e^{-jzx}}{z^4 + 4\beta^4} = 2\pi j \sum \text{residue's} \quad (6)$$

For positive x the contour is taken as in Fig. 3. The integrand becomes zero on the circle, when $R \rightarrow \infty$:

$$\oint_{R \rightarrow \infty} \frac{e^{-jzx}}{z^4 + 4\beta^4} = \int_{-\infty}^{-\infty} \frac{e^{-jsx}}{s^4 + 4\beta^4} ds \quad (7)$$

The poles are $z = \beta(1-j)$ and $z = -\beta(1+j)$

The function F_2 becomes:

$$\begin{aligned} F_2(x) &= \sqrt{2\pi} \left(\frac{e^{j\beta(1+j)x}}{1+j} + \frac{e^{-j\beta(1-j)x}}{1-j} \right) \frac{1}{8\beta^3} \\ &= \frac{1}{8\beta^3} \sqrt{2\pi} e^{-\beta x} (\cos \beta x + \sin \beta x) \\ &= \frac{1}{8\beta^3} \sqrt{2\pi} \varphi(\beta x) \end{aligned} \quad (9)$$

For physical reasons it is obvious that the function $F_2(x)$ is even

$$F_2(x) = \frac{1}{8\beta^3} \sqrt{2\pi} \varphi(|\beta x|) \quad (10)$$

The displacement field is thus given by the convolution integral:

$$u(x) = \frac{1}{2} \alpha \beta a \int_{-\infty}^{+\infty} T(\xi) \varphi(\beta |x-\xi|) d\xi \quad (11)$$

By partial integration (11) can be separated into a pure thermal dilatation displacement and into an elastic displacement.

$$\begin{aligned} u(x) &= \alpha a T + \frac{\alpha a}{4\beta} \int_{-\infty}^{+\infty} \frac{d^2 T(\xi)}{d\xi^2} \psi(\beta |x-\xi|) d\xi \\ \psi(\beta x) &= e^{-\beta x} (\cos \beta x - \sin \beta x) \end{aligned} \quad (12)$$

2. Relation between displacement and fluxes

Combining the differential equations governing the axial heat transport and the radial displacement, and applying the Fourier transform yields:

$$U(s) = \frac{4\beta^4 \alpha a m^2}{h} \frac{Q(s)}{(s^4 + 4\beta^4)(s^2 + m^2)} \quad (13)$$

The function $F_2(x)$ (see appendix 1) is now defined by:

$$F_2(x) = \frac{1}{\sqrt{2\pi}} \int_{-\infty}^{+\infty} \frac{e^{-jsx}}{(s^4 + 4\beta^4)(s^2 + m^2)} ds \quad (14)$$

This integral is calculated by contour integration :

$$\oint \frac{e^{-jzx}}{(z^4 + 4\beta^4)(z^2 + m^2)} dz = 2\pi j \Sigma \text{ residue's} \quad (15)$$

For positive x the contour is taken as in Fig. 3 and for $R \rightarrow \infty$ the integrand becomes zero on the circle:

$$\oint \frac{e^{-jzx}}{(z^4 + 4\beta^4)(z^2 + m^2)} dz = \int_{+\infty}^{-\infty} \frac{e^{-jsx}}{(s^4 + 4\beta^4)(s^2 + m^2)} ds \quad (16)$$

The poles are at $z = -jm$, $z = \beta(1-j)$ and $z = -\beta(1+j)$.

The function $F_2(x)$ becomes (still for positive x):

$$F_2(x) = \sqrt{2\pi} \left[\frac{e^{-mx}}{2m(m^4 + 4\beta^4)} + \frac{e^{j\beta(1+j)x}}{8\beta^3(1+j)(m^2 + 2j\beta^2)} + \frac{e^{-j\beta(1-j)x}}{8\beta^3(1-j)(m^2 - 2j\beta)} \right] \quad (17)$$

$$= \frac{\sqrt{2\pi}}{m^4 + 4\beta^4} \left[\frac{e^{-mx}}{2m} + \frac{m^2}{8\beta^3} \varphi(\beta x) - \frac{1}{4\beta} \psi(\beta x) \right]$$

Finally one obtains the following convolution integral for the displacement field $u(x)$:

$$\begin{aligned}
 u(x) = \frac{\alpha}{4} & \frac{1}{1+4\left(\frac{\beta}{m}\right)^4} \left\{ 2 \int_{-\infty}^{+\infty} q(\xi) \varphi(\beta|x-\xi|) d\xi \right. \\
 & - 4 \int_{-\infty}^{+\infty} q(\xi) \psi(\beta|x-\xi|) d\xi \\
 & \left. + \left(\frac{\beta}{m}\right)^5 \int_{-\infty}^{+\infty} \dot{q}(\xi) e^{-m|x-\xi|} d\xi \right\} \quad (18)
 \end{aligned}$$

In formula 1 of chapter 4 the thermal dilatation displacement has been separated:

$$u_{\text{th}} = \alpha \Delta \vartheta = \int_{-\infty}^{+\infty} q(\xi) e^{-m|x-\xi|} d\xi \quad (19)$$

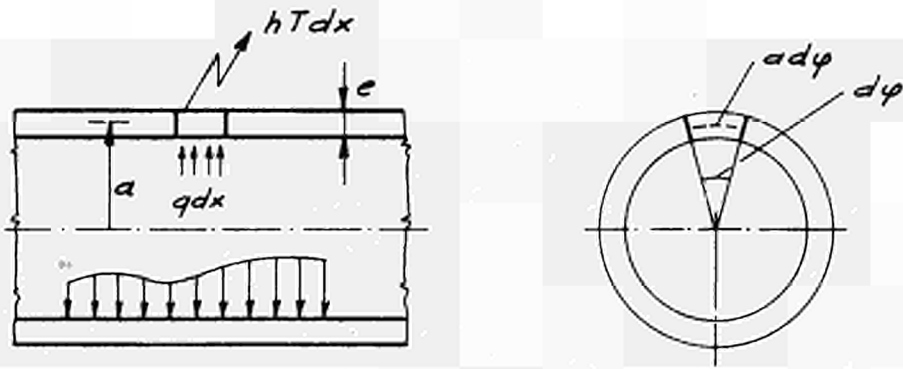


Fig. 1

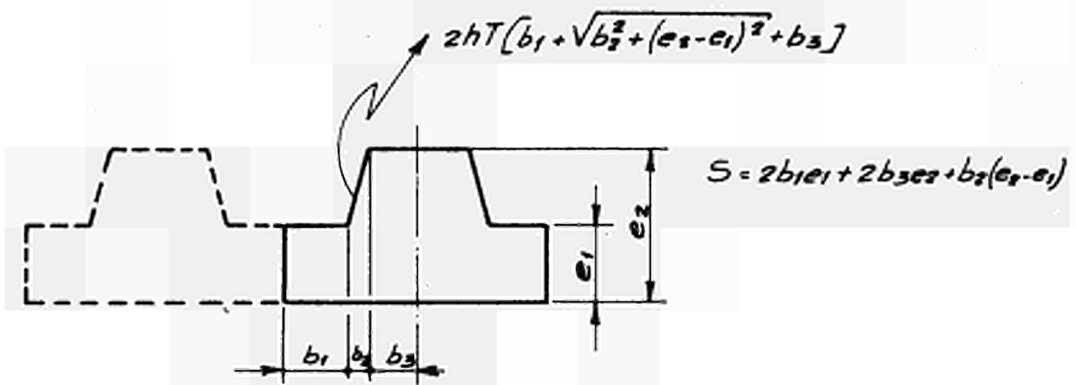


Fig. 2

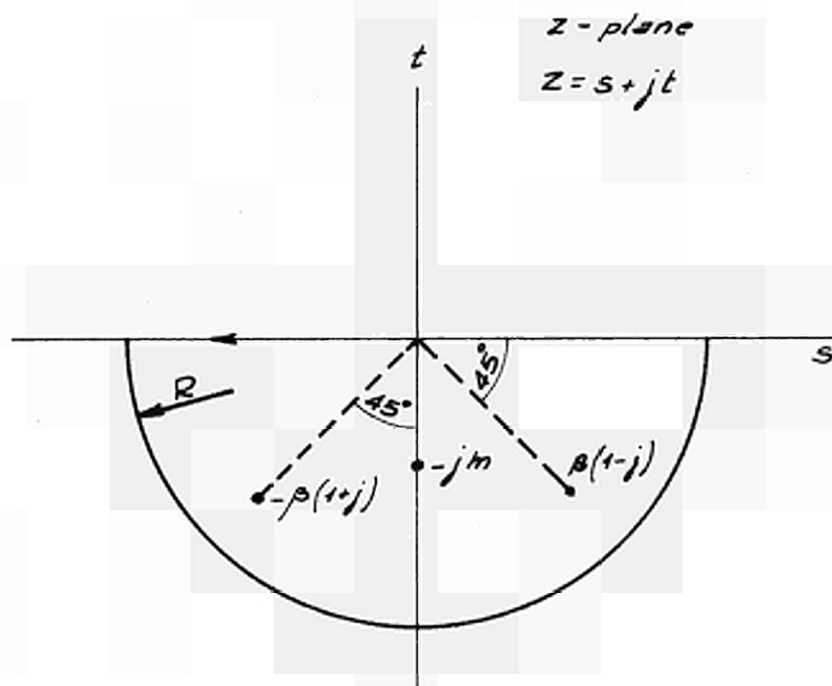


Fig. 3

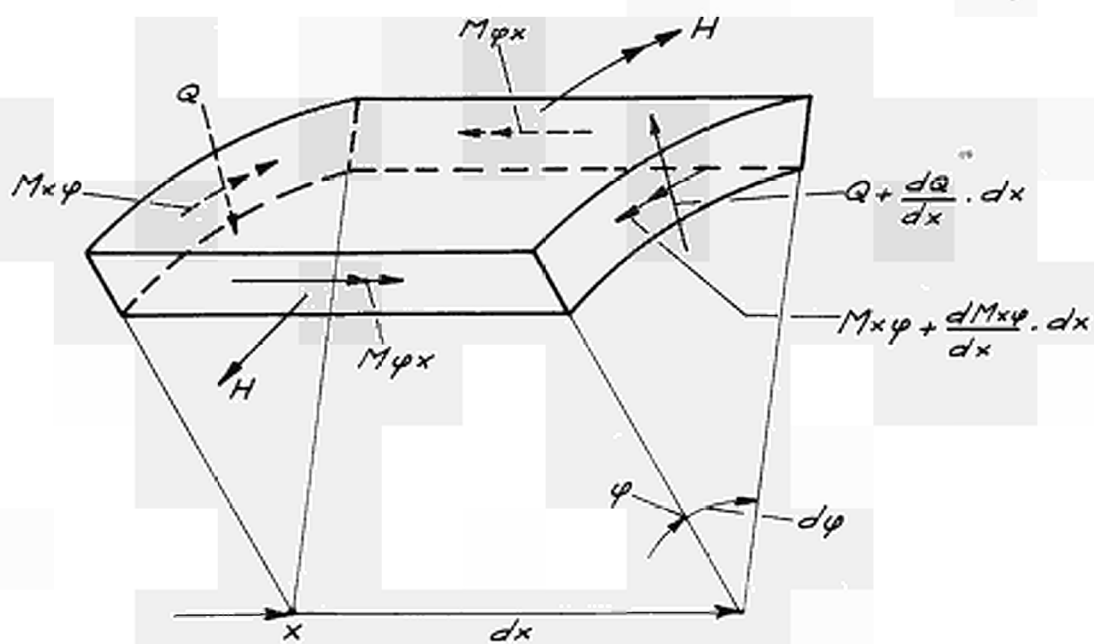


Fig. 4

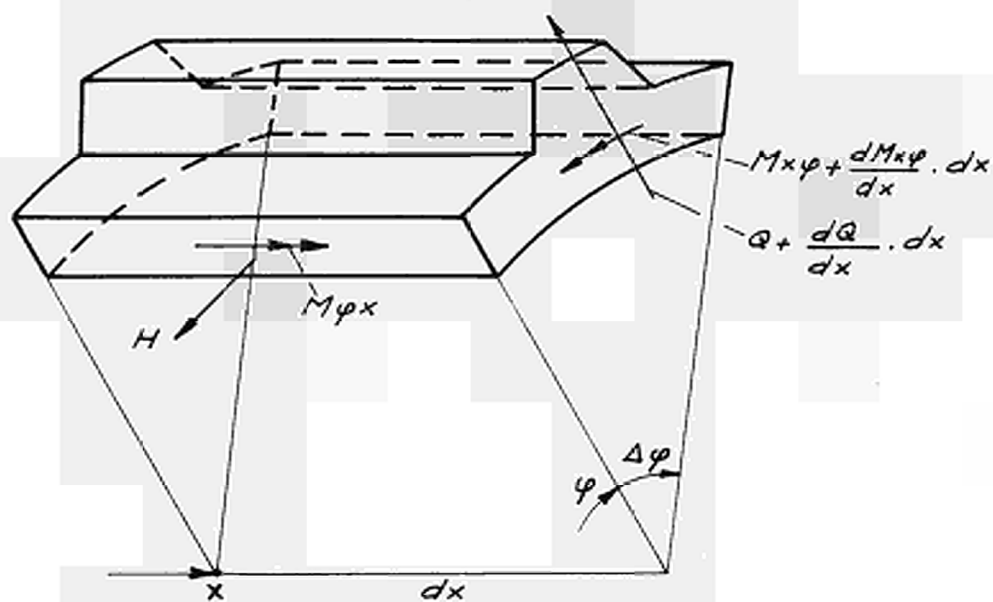


Fig. 5

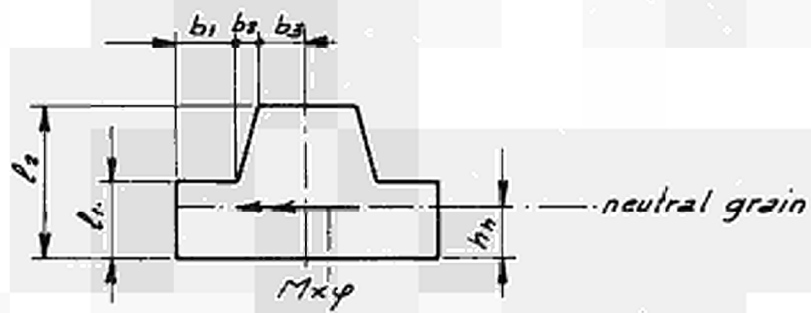


Fig. 6



Fig. 7



Fig. 8

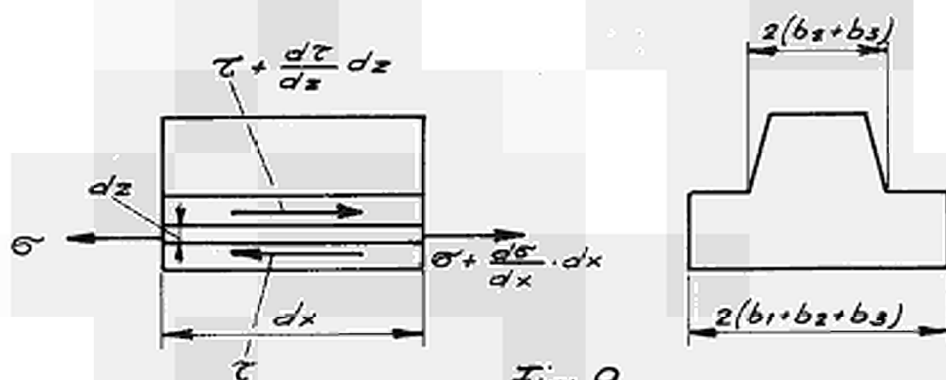


Fig. 9

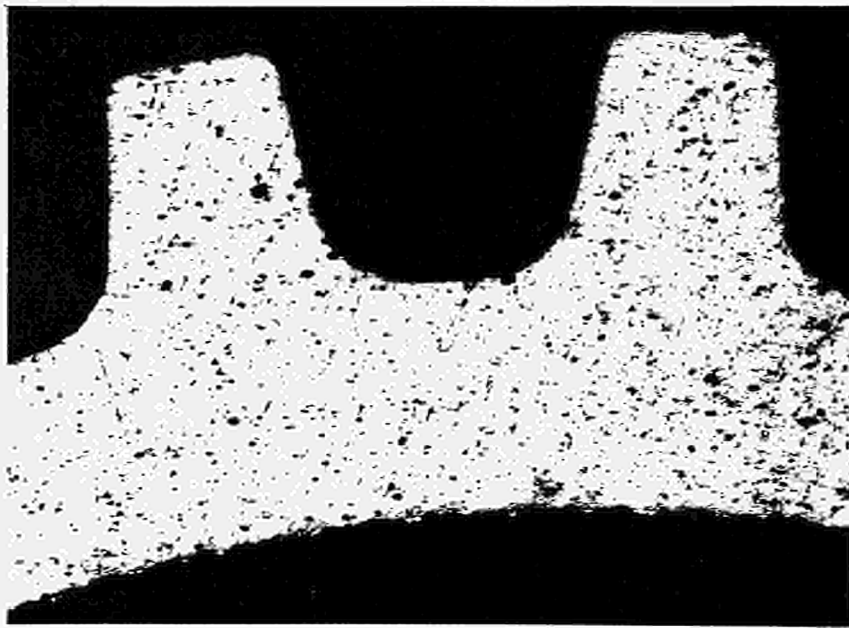
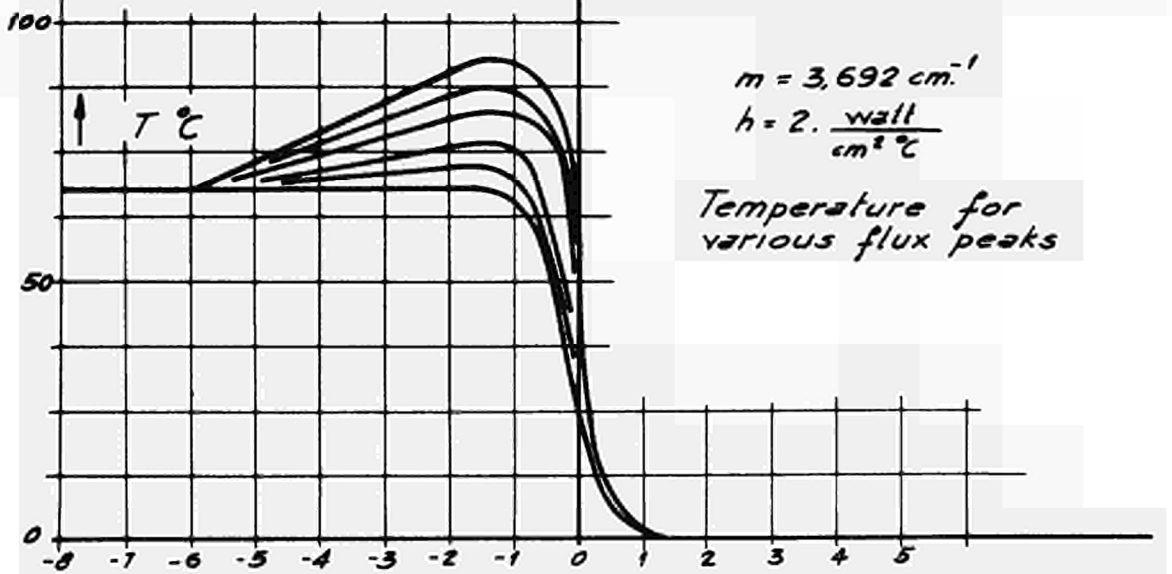
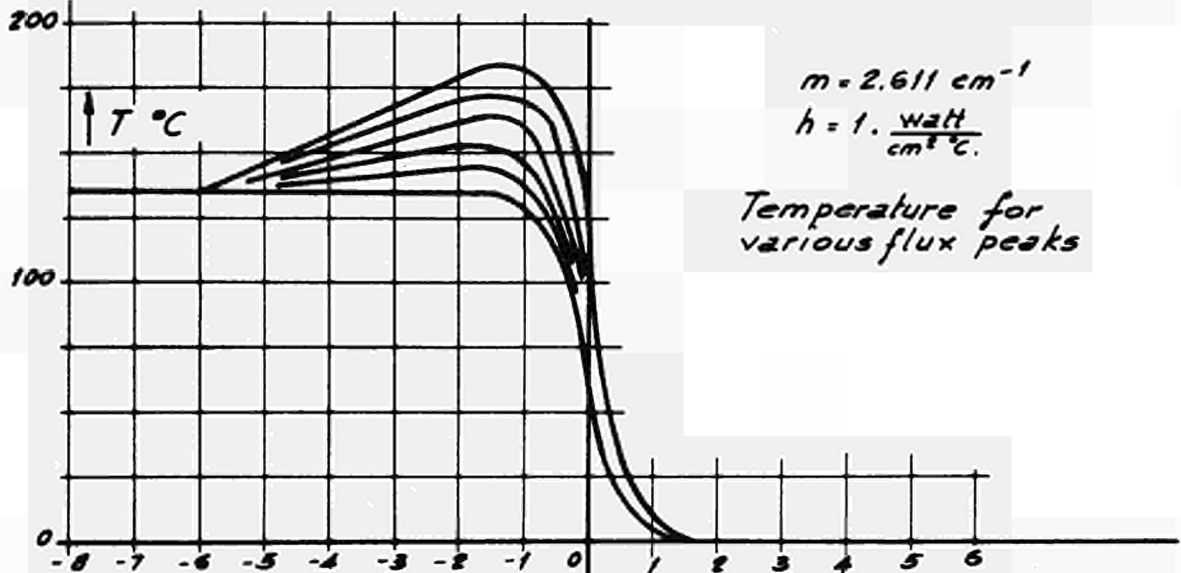
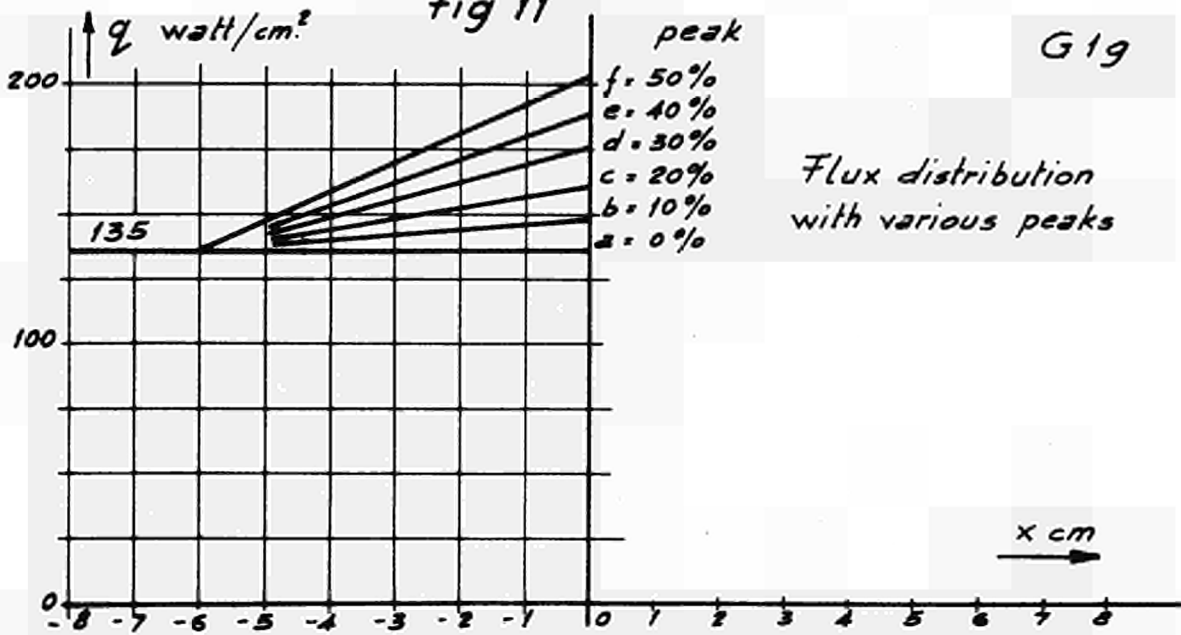
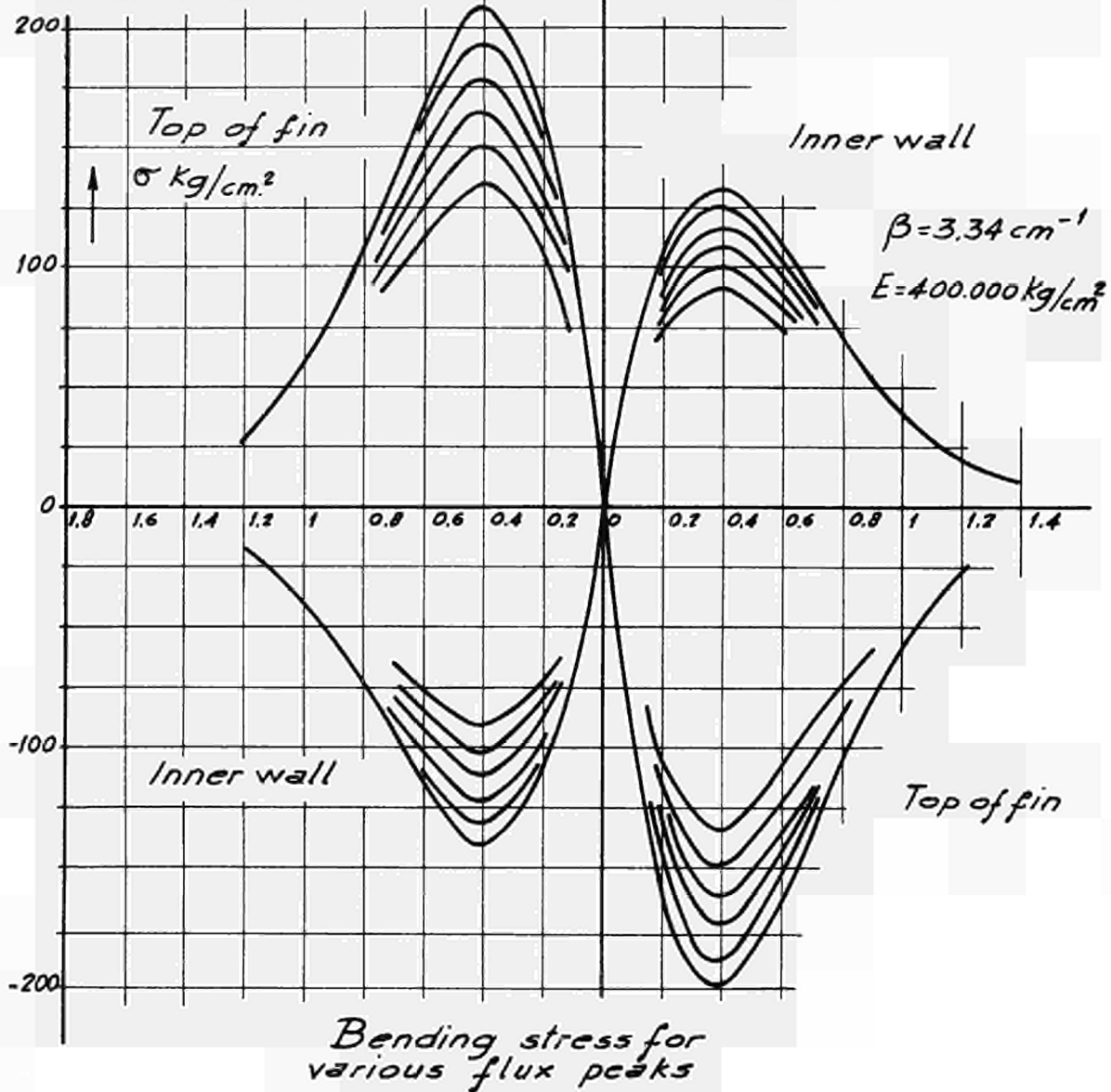
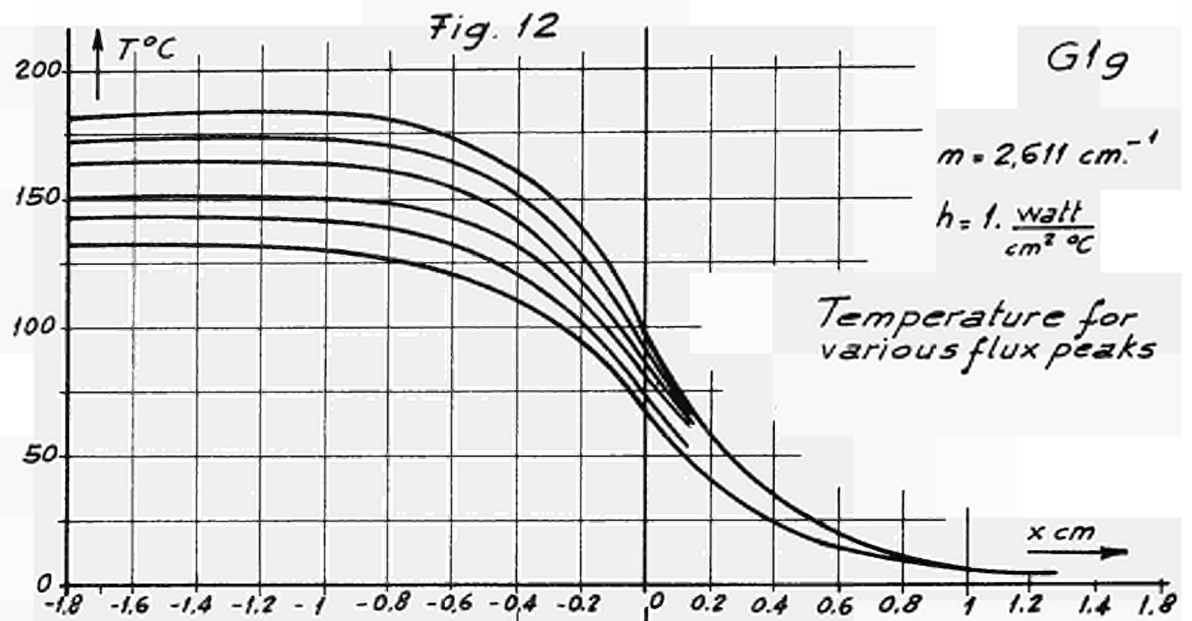


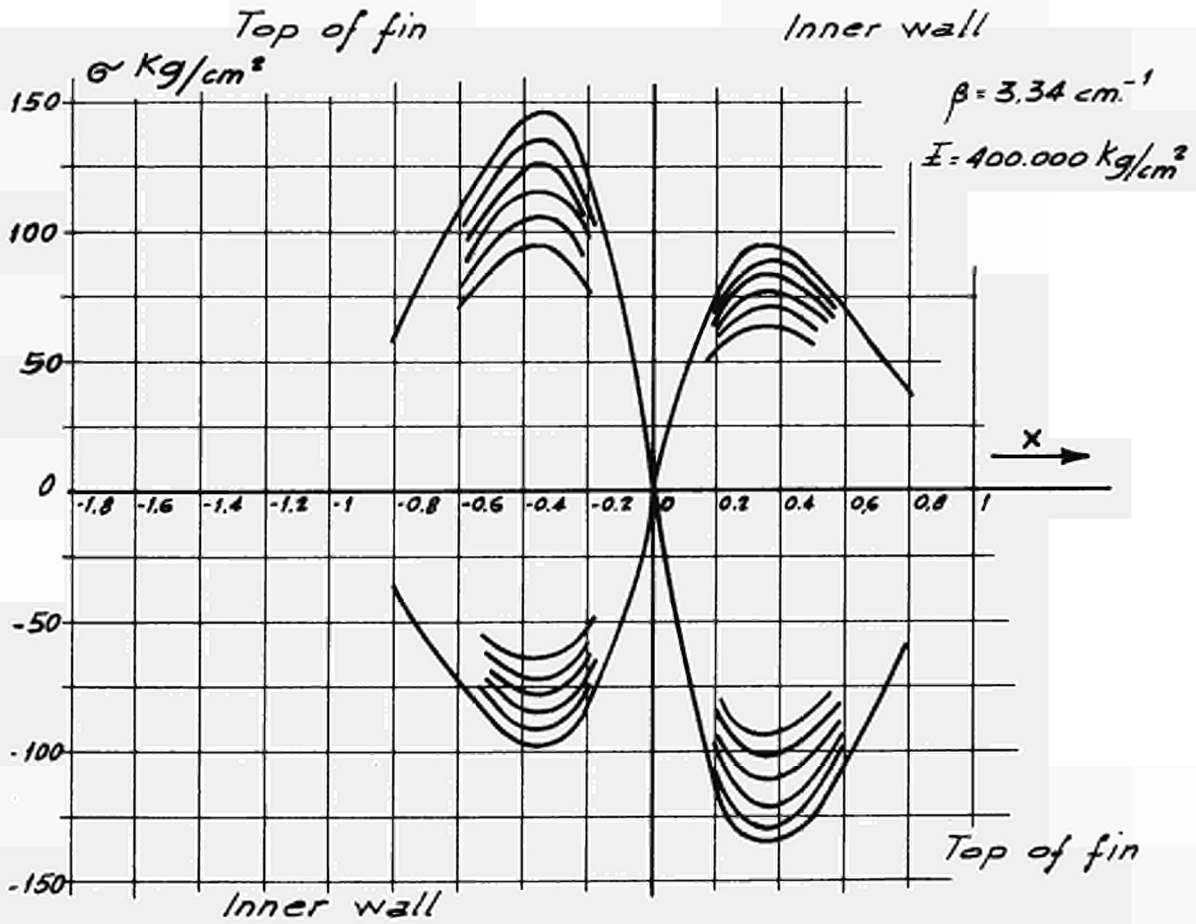
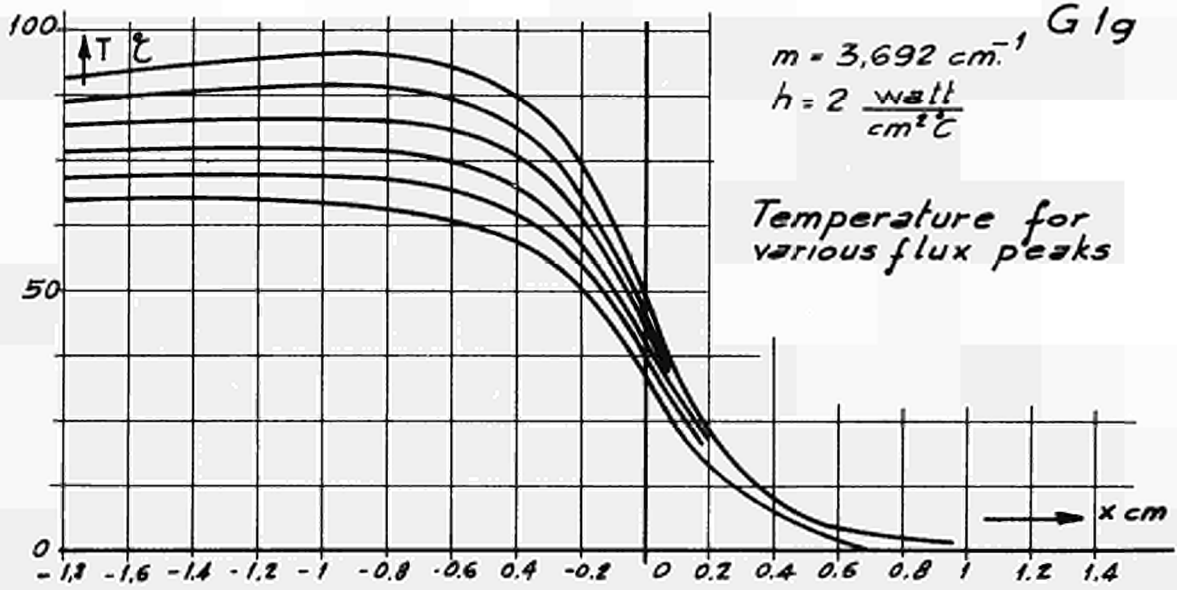
Fig. 10
enlarged photograph of a G 19
finned canning wall

Fig 11

G 19







Bending stress for various flux peaks

Fig. 13

Fig. 14

Equivalent stress in corner of fin according to Huber deformation energy criterion

$$\sigma_e = \sqrt{\frac{1}{2} \{ (\sigma_1 - \sigma_2)^2 + (\sigma_2 - \sigma_3)^2 + (\sigma_3 - \sigma_1)^2 \}}$$

$$q = 135 \text{ watt/cm}^2$$

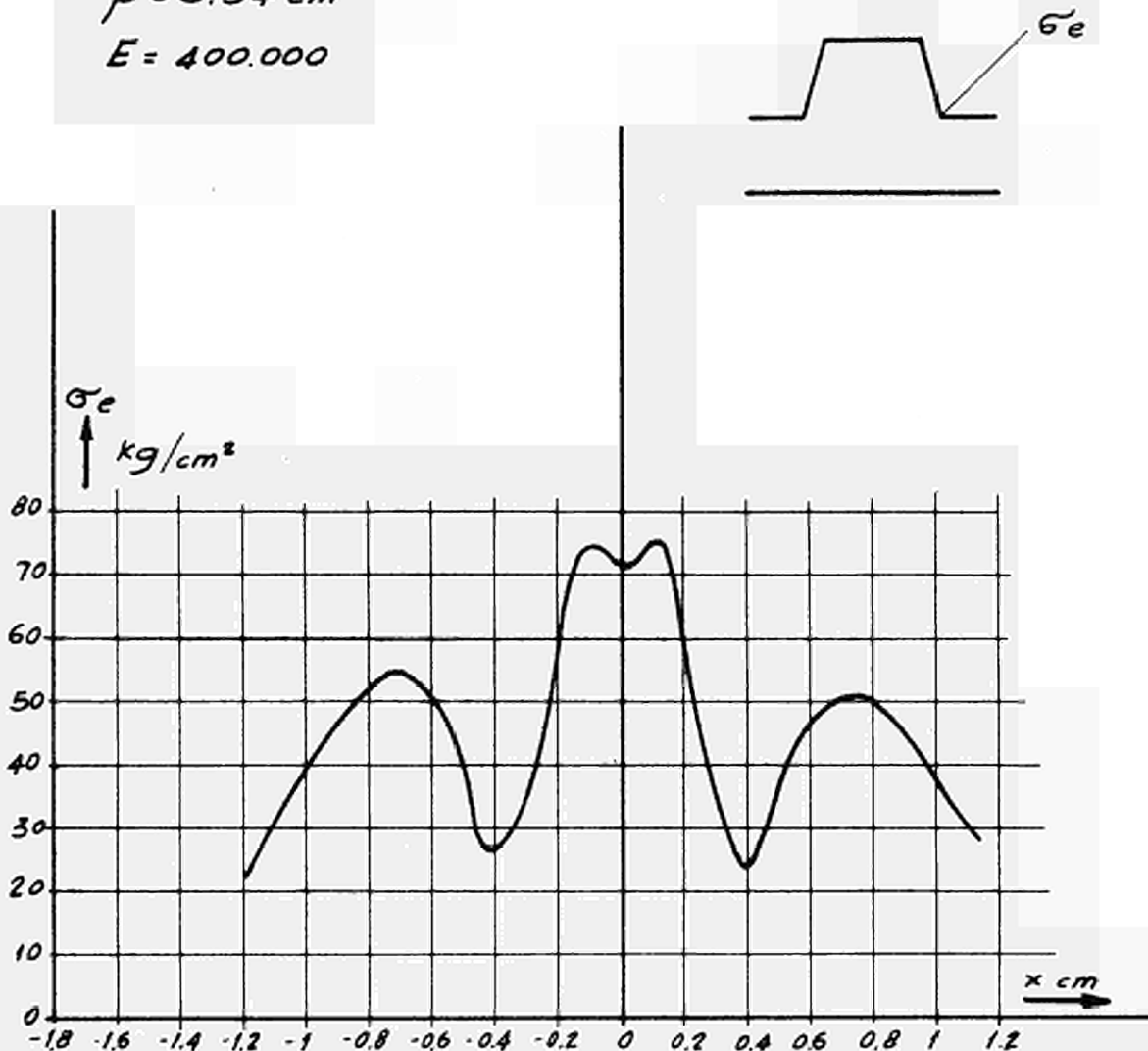
Peak 50%

$$h = 1 \text{ watt/cm}^2\text{°C}$$

$$m = 2.611 \text{ cm}^{-1}$$

$$\beta = 3.34 \text{ cm}^{-1}$$

$$E = 400.000$$



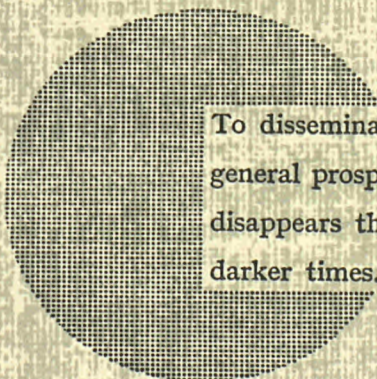
NOTICE TO THE READER

All Euratom reports are announced, as and when they are issued, in the monthly periodical **EURATOM INFORMATION**, edited by the Centre for Information and Documentation (CID). For subscription (1 year : US\$ 15, £ 5.7) or free specimen copies please write to :

Handelsblatt GmbH
"Euratom Information"
Postfach 1102
D-4 Düsseldorf (Germany)

or

Office central de vente des publications
des Communautés européennes
2, Place de Metz
Luxembourg



To disseminate knowledge is to disseminate prosperity — I mean general prosperity and not individual riches — and with prosperity disappears the greater part of the evil which is our heritage from darker times.

Alfred Nobel

SALES OFFICES

All Euratom reports are on sale at the offices listed below, at the prices given on the back of the front cover (when ordering, specify clearly the EUR number and the title of the report, which are shown on the front cover).

OFFICE CENTRAL DE VENTE DES PUBLICATIONS DES COMMUNAUTES EUROPEENNES

2, place de Metz, Luxembourg (Compte chèque postal N° 191-90)

BELGIQUE — BELGIË

MONITEUR BELGE
40-42, rue de Louvain - Bruxelles
BELGISCH STAATSBLAD
Leuvenseweg 40-42 - Brussel

LUXEMBOURG

OFFICE CENTRAL DE VENTE
DES PUBLICATIONS DES
COMMUNAUTES EUROPEENNES
9, rue Goethe - Luxembourg

DEUTSCHLAND

BUNDESANZEIGER
Postfach - Köln 1

NEDERLAND

STAATSDRUKKERIJ
Christoffel Plantijnstraat - Den Haag

FRANCE

SERVICE DE VENTE EN FRANCE
DES PUBLICATIONS DES
COMMUNAUTES EUROPEENNES
26, rue Desaix - Paris 15^e

ITALIA

LIBRERIA DELLO STATO
Piazza G. Verdi, 10 - Roma

UNITED KINGDOM

H. M. STATIONERY OFFICE
P. O. Box 569 - London S.E.1

EURATOM — C.I.D.
51-53, rue Belliard
Bruxelles (Belgique)

CDNA03557ENC